Derivation of an Interatomic Potential for Germanium- and Silicon-Containing Zeolites and Its Application to the Study of the Structures of Octadecasil, ASU-7, and ASU-9 Materials

German Sastre[†] and Julian D. Gale*[,‡]

Instituto de Tecnologia Quimica U.P.V.-C.S.I.C, Universidad Politecnica de Valencia, Avenida Los Naranjos s/n, 46022 Valencia, Spain, and Department of Chemistry, Imperial College of Science, Technology and Medicine, South Kensington, SW7 2AZ London, U.K.

Received July 17, 2002. Revised Manuscript Received January 6, 2003

An interatomic potential for Ge/Si-zeolites has been developed by fitting to the experimental properties of quartz, GeO_2(quartz), and GeO_2(rutile). Testing the force field by comparison of the experimental and computed structural properties of octadecasil, ASU-7, and ASU-9 shows errors within 1−2% in the cell parameters and interatomic distances. Furthermore, Ge−O−Ge angles are well reproduced and predicted to lie within the range of 130−138° as compared to the experimental values in the range 126−140°. The force field can be used for new zeotype structures containing germanium and silicon as tetrahedral atoms in order to predict structural properties, as well as the energetic stability of different Ge and Si orderings. Improved accuracy is achieved, relative to earlier force fields, through the use of different polarizabilities for the oxide ion in distinct environments.

1. Introduction

New silica-based zeolite structures require for their synthesis the use of additives that stabilize particular frameworks among a number of possible phases.[1,2] Apart from the use of organic species that provide a favorable energetic interaction with the micropore neighborhood, some inorganic elements have recently been found to direct the synthesis. For example, the use of fluoride instead of hydroxide as the mineralizing agent has allowed the synthesis of silica zeolites with rather low densities,[3] and the use of germanium in the synthesis gel favors the formation of zeolite structures containing double four rings (D4R), such as ITQ-7,[4,5] and Beta-C.[6,7] Substitution of Si by Ge is one of the most isomorphic examples in four-connected nets due to the tetravalent character of both species and the fact that there is no net charge to be compensated in the framework after the substitution. The different chemical behavior of Si and Ge yields a more ionic character for Ge networks as well as larger T−O distances (1.613 and 1.738 Å for T = Si and Ge, respectively, in quartz-like phases). Furthermore, a lower Ge−O−Ge angle with respect to Si−O−Si is expected from the similar Ge−Ge and Si−Si distances (3.15 and 3.05 Å for GeO_2 and SiO_2, respectively, in quartz-like structures.

The differences between Si and Ge in zeolites can also be studied in the light of the behavior of the corresponding SiO_2 and GeO_2 polymorphs (silica and germania). The stable form of silica at ambient temperature and pressure is α-quartz (hereafter called Si-q), which transforms into coesite and stishovite (six-coordinated Si) under increasing pressure. At high temperature, phases such as crystobalite and tridymite are obtained. On the other hand, only two stable phases of germania are found at ambient temperatures, based on the quartz (Ge-q) and rutile (Ge-r) structures, the latter being the more stable and isomorphous to stishovite. The rutile-like phase is stable at ambient conditions and transforms into Ge-q at 1280 K under atmospheric pressure.[8] The more stable 6-fold coordination for germanium dictates that, initially, microporous germanates were a combination of tetrahedral, trigonal bipyramidal, and/or octahedral coordinations.[9−12] The first transformation of germania into a microporous four-connected framework was reported recently by Li and Yaghi[13] who obtained the ASU-7 and ASU-9 materials with the

* To whom correspondence should be addressed. Phone: +44-20-7594-5757. Fax: +44-20-7594-5850. E-mail: j.gale@ic.ac.uk.
[†] Universidad Politecnica de Valencia.
[‡] Imperial College of Science, Technology and Medicine.

(1) Davis, M. E.; Lobo, R. F. *Chem. Mater.* **1992**, *4*, 756.
(2) Petrovic, I.; Navrotsky, A.; Davis, M. E.; Zones, S. I. *Chem. Mater.* **1993**, *5*, 1805.
(3) Piccione, P. M.; Laberty, C.; Yang, S.; Camblor, M. A.; Navrotsky, A.; Davis, M. E. *J. Phys. Chem. B* **2000**, *104*, 10001.
(4) Villaescusa, L. A.; Barrett, P. A.; Camblor, M. A. *Angew. Chem., Int. Ed.* **1999**, *38*, 1997.
(5) Corma, A.; Diaz-Cabañas, M. J.; Fornes, V. *Angew. Chem., Int. Ed.* **2000**, *39*, 2346.
(6) Corma, A.; Navarro, M. T.; Rey, F.; Rius, J.; Valencia, S. *Angew. Chem., Int. Ed.*. **2001**, *40*, 2277.
(7) Corma, A.; Navarro, M. T.; Rey, F.; Valencia, S. *Chem. Commun.* **2001**, 1486.
(8) Hill, V. G.; Chang, L. L. Y. *Am. Mineral.* **1968**, *53*, 1744.
(9) Roberts, M. A.; Fitch, A. N. Z. *Kristallografiya* **1996**, *211*, 378.
(10) Jones, R. H.; Chen, J.; Thomas, J. M.; George, A.; Hursthouse, M. B.; Xu, R.; Li, S.; Lu, Y.; Yang, G. *Chem. Mater.* **1992**, *4*, 808.
(11) Cheng, J. C.; Xu, R.; Yang, G. J. *Chem. Soc. Dalton Trans.* **1991**, 1537.
(12) Cascales, C.; Gutierrez-Puebla, E.; Monge, M. A.; RuizValero, C. *Angew. Chem., Int. Ed.* **1998**, *37*, 129.
(13) Li, H.; Yaghi, O. M. *J. Am. Chem. Soc.* **1998**, *120*, 10569.

10.1021/cm021262y CCC: $25.00
Published on Web 04/10/2003

Table 1. Coordination Sequences and Vertex Symbols of the ASU-7 and ASU-9 Structures as Determined Using ZeoTsites[46]

ASU-7

Coordination Sequence													
Ge1 (4)	4	12	18	26	52	84	100	118	162	210	248	284	332
Ge2(16)	4	9	19	35	52	72	100	131	163	201	244	290	340
Vertex Symbols													
Ge1	6_1	6_1	6_2	6_2	12_8	12_8							
Ge2	4_1	6_1	4_1	6_1	4_1	6_1							

ASU-9

Coordination Sequence													
Ge1(16)	4	9	19	34	48	66	96	127	151	183	232	281	316
Ge2 (4)	4	12	18	28	52	78	88	112	162	204	220	254	328
Vertex Symbols													
Ge1	4_1	6_1	4_1	6_1	4_1	6_1							
Ge2	6_1	6_1	6_1	6_1	6_1	6_1							

topology characterized by the coordination sequences[14] and vertex symbols[15] shown in Table 1. ASU-9 corresponds to the International Zeolite Association (IZA) code AST,[16] whereas ASU-7 has been assigned the code ISV. The existence of a siliceous counterpart in the case of ASU-9, this being octadecasil, means that, as in the case of quartz, there is a range of T−O−T angles that can be accommodated by both elements, or that the common structural types (quartz, AST) are flexible enough to accommodate equilibrium angles for Si−O−Si and Ge−O−Ge. On the other hand, no silica analogue of ASU-7 has yet been found and a structural analysis of the geometry changes relative to the germania counterpart could yield information as to the viability of its synthesis.

The use of computer simulations can be of valuable help in understanding the relative stabilities of different phases through the calculation of the framework energies of these new materials with the pure germania and silica compositions, as well as for intermediate phases where Ge is doped into the silica framework. In this latter case, preferential locations for germanium could be established from the calculation of the relative energies of the statistically sampled distributions over the entire compositional range of Si/Ge ratios. Finally, this methodology could also be applied to zeolitic materials synthesized with both Si and Ge, such as the recent cases of ITQ-7 and Beta-C, to find the preferred locations of each cation. Aside from using first principles calculations,[17−19] the interatomic potential approach has also rendered valuable results[20−22] and it can be more conveniently applied when a large number of possibilities has to be explored because of its significantly lower computational expense. To be successful as a predictive tool, it is essential to ensure that the force field is of the highest possible quality. In this work, we present a new force field for Si/Ge zeolites that has been parametrized by taking into account a larger set of structures than previous models[23,24] in order to maximize transferability.

2. Methodology

2.1. Potential Fitting. Empirical fitting consists of minimizing the difference between observed and calculated properties by means of a least squares procedure. Concurrent fitting of multiple structures is found to greatly enhance the reliability of the derived potentials and generally leads to more physically reasonable potentials without the use of constraints. In our case, we are interested in Si/Ge-based zeolites and therefore we have included in the fit the structures of silica and germania. The structures of Si-q[25] and Ge-q[26] are both included as observables. An important issue here is the fact that Ge-zeolites are four-connected germania networks, despite the fact that Ge cations tend toward 6-fold coordination. This is demonstrated by the greater stability of the rutile analogue with respect to Ge-q, and therefore this ground-state structure[27] has also been included in the observables, thus leading to three structures being included in the concurrent fit. Beyond the structure, it is also vital to incorporate data regarding the curvature of the energy surface about the minima. Hence, apart from the structures, the other observables included are the bulk moduli (of Si-q, Ge-q, and Ge-r), as well as the elastic constants and the highest phonon frequency (of Si-q). Table 2 contains all the observables used within the fit.

In the present work, the relaxed fitting scheme[28] is employed for the final refinement of the potential parameters, as implemented in the program GULP.[29] Here the structure of every phase is minimized at each point of the least-squares procedure, and the displacements from the experimentally observed structure form the basis of the residuals, instead of just using the forces acting on the structure at the experimental geometry. Similarly, the curvature related properties are evaluated at the optimized structure because this is more reliable and formally correct.

The potential model used is the Born model with inclusion of dipolar polarization of oxygen, as was done in most previous work,[30] and consists of the Coulomb interaction, evaluated via an Ewald summation, a short-range pair potential described by a Buckingham function with cutoff distance of 12 Å, and a three-body angle

(14) (a) Meier, W. M.; Moeck, H. J. *J. Solid State Chem.* **1979**, *27*, 349. (b) Brunner, G. O. *J. Solid State Chem.* **1979**, *29*, 41.
(15) O'Keeffe, M.; Hyde, S. T. *Zeolites* **1997**, *19*, 370.
(16) Baerlocher, Ch.; Meier, W. M.; Olson, D. H. *Atlas of Zeolite Structure Types*, 5th revised ed.; Elsevier: Amsterdam, The Netherlands, 2001. Also http://www.iza-structure.org.
(17) Jolly, L. H.; Silvi, B.; Darco, P. *Eur. J. Miner.* **1994**, *6*, 7.
(18) Christie, D. M.; Chelikowsky J. R. *Phys. Rev. B* **2000**, *62*, 14703.
(19) Blasco, T.; Corma, A.; DíazCabañas, M. J.; Rey, F.; VidalMoya, J. A.; ZicovichWilson, C. M. *J. Phys. Chem. B* **2002**, *106*, 2634.
(20) Catlow, C. R. A., Mackrodt, W. C., Eds.; *Computer Simulations of Solids*; Lecture Notes in Physics, 166, ; Springer-Verlag: Berlin, 1982.
(21) Catlow, C. R. A., Ed.; *Modelling of Structure and Reactivity in Zeolites*; Academic Press: London, 1992.
(22) Catlow, C. R. A.; Bell, R. G.; Gale, J. D. *J. Mater. Chem.* **1994**, *4*, 781.
(23) George, A. R.; Catlow, C. R. A. *Zeolites* **1997**, *18*, 67.
(24) Tsuchiya, T.; Yamanaka, T.; Matsui, M. *Phys. Chem. Miner.* **1998**, *25*, 94.
(25) Bolzan, A. A.; Fong, C.; Kennedy, B. J.; Howard, C. J. *Acta Crystallogr. B* **1997**, *53*, 373.
(26) Lager, G. A.; Jorgensen, J. D.; Rotella, F. J. *J. Appl. Phys.* **1982**, *53*, 6751.
(27) Glinnemann, J.; King, H. E., Jr.; Schulz, H.; Hahn, Th.; La Placa, S. J.; Dacol, F. *Z. Kristallogr.* **1992**, *198*, 177.
(28) Gale, J. D. *Philos. Magaz. B* **1996**, *73*, 3.
(29) Gale, J. D. *J. Chem. Soc., Faraday Trans.* **1997**, *93*, 629.
(30) (a) Sanders, M. J.; Leslie, M.; Catlow, C. R. A. *J. Chem. Soc, Chem. Commun.* **1984**, 1271. (b) Jackson, R. A.; Catlow, C. R. A. *Mol. Simul.* **1988**, *1*, 207.

bending term (O−Si−O). The shell model was used to simulate the polarizability of the oxygen ions. For the germanium-containing structures, the three-body bending term was omitted based on our previous observation above that 6-fold as well as 4-fold coordinated structures are taken into account in the fit. The functional forms are as follows:

$$E^{silica} = E^{Buckingham} + E^{threebody} + E^{core-shell} + E^{Coulombic} \quad (1)$$

$$E^{germania} = E^{Buckingham} + E^{core-shell} + E^{Coulombic} \quad (2)$$

$$E_{ij}^{Buckingham} = A_{ij} \exp\left(-\frac{r_{ij}}{\rho_{ij}}\right) - \frac{C_{ij}}{r_{ij}^6} \quad (3)$$

$$E_{ijk}^{threebody} = \frac{1}{2}k_{ijk}(\theta - \theta_0)^2 \quad (4)$$

$$E_{ij}^{core-shell} = \frac{1}{2}k_{ij}^{cs}r_{ij}^2 \quad (5)$$

$$E_{ij}^{Coulombic} = \frac{q_i q_j}{4\pi\epsilon_0 r_{ij}} \quad (6)$$

In modeling oxide materials, the shell model for the oxygen atoms has proven essential in order to fit dielectric constants, phonons, and other characteristic properties. This is because the polarization of oxygen may also act to mimic covalency effects that would lead to lower ionic charges than the formal ones, which are chosen in the present study, and many previous ones. This can be demonstrated through the calculation of the Born effective charge tensor for the shell model, which yields on-diagonal charges of the order of +3 for Si using the model of Sanders et al. The oxygen core−shell charge split and force constant, which determine the polarizability, as well as the oxygen−oxygen short-range interaction, have long retained the parameters derived when the original force field for α-quartz was fitted[30] and no modification was made when this work was extended to include microporous aluminophosphates.[31] This represents an important feature, leading to transferability of this potential, which has allowed a consistent treatment of microporous materials containing any mixture of Si, Al, or P as tetrahedral atoms.[32]

2.2. Energy Minimization. Once the parametrization is completed, energy minimizations were performed in order to examine the ability of the force field to reproduce the structures of octadecasil,[33] ASU-7, and ASU-9,[13] which were not included in the original fit, thereby providing a test of the transferability. Apart from the zeolite force field, already described, the terms including the template molecule and its interaction with the zeolite are also necessary when the experimental XRD structure has been solved for noncalcined materials, as is the case for octadecasil, ASU-7, and ASU-9. Octadecasil has also been solved after calcination[29] and this is further included in the test. The total potential energy function and the respective terms are as follows:

$$E^{total} = E^{zeolite} + E^{complex} + E^{zeolite-complex} + E^{complex-complex} \quad (7)$$

The $E^{zeolite}$ term has already been described in eqs 1−6 and the other terms are as follows:

$$E^{complex} = E^{harmonic} + E^{threebody} + E^{torsion} + E^{Coulombic} \quad (8)$$

$$E^{zeolite-complex} = E^{Lennard-Jones} + E^{Coulombic} \quad (9)$$

$$E^{complex-complex} = E^{Lennard-Jones} + E^{Coulombic} \quad (10)$$

Three-body and Coulombic terms have already been described in eqs 4 and 6, and the other terms are as

Table 2. Comparison of the Experimental and Calculated Structure and Properties of Ge-q, Ge-r, and Si-q

	experimental	calculated
Ge-q		
a (Å)	4.9845	4.9860
c (Å)	5.6477	5.6581
Ge(*x*)	0.4513	0.4484
O(*x*)	0.3965	0.4061
O(*y*)	0.3022	0.3042
O(*z*)	0.2422	0.2401
cell volume (Å^3)	121.519	121.817
bulk modulus (GPa)	36.0	37.7
Ge−O (Å)	1.738	1.724
Ge−Ge (Å)	3.152	3.158
Ge−O−Ge (°)	130.0	132.7
O−Ge−O (°)	113.2	111.5
	107.6	111.0
	106.3	105.7
	106.3	106.0
	110.3	111.3
	113.2	111.5
Ge-r		
a (Å)	4.4066	4.3194
c (Å)	2.8619	2.9716
O(*x*)	0.3060	0.3118
cell volume (Å^3)	55.573	55.441
bulk modulus (GPa)	258.0	242.8
Ge−O (Å)	1.873	1.879
	1.907	1.905
Si-q		
a (Å)	4.9021	4.9040
c (Å)	5.3997	5.4156
Si(*x*)	0.4680	0.4698
O(*x*)	0.4124	0.4125
O(*y*)	0.2712	0.2686
O(*z*)	0.2170	0.2160
cell volume (Å^3)	112.374	112.792
C_{11} (GPa)	86.80	97.64
C_{12} (GPa)	7.04	15.84
C_{13} (GPa)	11.91	23.97
C_{14} (GPa)	−18.04	−14.52
C_{33} (GPa)	105.75	113.58
C_{44} (GPa)	58.20	50.50
C_{66} (GPa)	39.90	40.90
ϵ_{11} (static)	4.52	4.85
ϵ_{33} (static)	4.64	5.20
ϵ_{11} (high freq.)	2.40	2.06
ϵ_{33} (high freq.)	2.40	2.08
maximum frequency at Γ (cm^{-1})	1162	1118
Si−O (Å)	1.613	1.612
Si−Si (Å)	3.053	3.056
Si−O−Si (°)	142.4	142.9
O−Si−O (°)	110.7	110.7
	108.9	108.5
	108.6	108.5
	108.6	108.6
	109.4	109.7
	110.7	110.7

(31) Gale, J. D.; Henson, N. J. *J. Chem. Soc., Faraday Trans.* **1994**, *90*, 3175.
(32) Sastre, G.; Lewis, D. W.; Catlow, C. R. A. *J. Phys. Chem.* **1996**, *100*, 6722.
(33) Caullet, P.; Guth, J. L.; Hazm, J.; Lamblin, J. M. *Eur. J. Solid State Inorg. Chem.* **1991**, *28*, 345.

follows:

$$E_{ij}^{harmonic} = \frac{1}{2}k_{ij}^{h}(r_{ij} - r_{ij}^{0})^2 \quad (11)$$

$$E_{ijkl}^{torsion} = k_{ijkl}^{t}[1 + \cos(n\phi - \phi_0)] \quad (12)$$

$$E_{ij}^{Lennard-Jones} = \frac{B_{ij}^{LJ}}{r_{ij}^{12}} - \frac{C_{ij}^{LJ}}{r_{ij}^{6}} \quad (13)$$

The force field by Kiselev et al.[35] was selected for the intermolecular template−zeolite and template−template interactions, for which it has been used successfully previously, while the force field by Oie et al.[36] was used to provide the remaining intramolecular interactions between the atoms of the template—a task to which it is well suited, having been designed to reproduce a wide range of organic crystal structures. The templates used in the synthesis of octadecasil, ASU-7, and ASU-9 are quinuclidine, DMA, and DABCO in their protonated forms, respectively. Quinuclidine is 1-azabicyclo [2.2.2] octane; DMA is dimethylamine; and DABCO is 1,4-diazabicyclo [2.2.2] octane. To treat in a realistic way the electrostatics of the interaction between the template and the zeolite, and between template molecules, previous full optimizations of the charged templates have been carried out at the ab initio Hartree−Fock level with the 6-31G** basis set, using the program NWChem.[37] The corresponding charges are listed in Table 4. Finally, the positive charge introduced by the presence of the template is compensated by inclusion of fluoride anions, thus resembling the synthesis conditions. The force field by George and Catlow[23] has been used to treat the interaction of fluoride with the zeolite.

3. Results

3.1. Force Field Derivation for GeO_2/SiO_2. There have been several previous attempts to extend the Sanders et al force field for silicates to other microporous framework materials, including for aluminophosphates[31] and gallophosphates,[38] as well as for germania itself. In these previous works, the approach taken has been to preserve the already defined aluminosilicate force field as unchanged, and to fit only the potential parameters that are left unconstrained by this requirement. For instance, in the case of the fit to berlinite the only two free parameters were the A and ρ of the P−O Buckingham potential, because all O−O and Al−O interactions were predetermined. In the case of aluminophosphates, this constraint resulted in few adverse effects on the quality of the fit. However, in subsequent studies on a wider range of materials this philosophy has proved problematic. For example, in the case of gallium phosphate it was impossible to obtain an adequate description of both bond lengths and Ga−O−P bond angles by varying only the Ga−O potential parameters. This necessitated the use of an additional Ga−P short-range potential to partially correct this deviation.[38] The same difficulty in simultaneously reproducing the Ge−O bond lengths and Ge−O−Ge bond angles is also found to occur for the germania analogue of quartz.

The above conflict between the optimal parameters for SiO_2 and GeO_2 can be traced to the differing ionic character of the two materials. However, because both are treated as fully ionic in order to make defect problems facile to study this must be compensated through the shell model parameters. Hence, we can conclude that the essence of the solution is that the polarizability of oxygen within the shell model must be different for silica and germania. The question is how to reconcile this with the need for compatibility of force fields so as to be able to treat impurities of one atom within the framework of the other? Consequently, we have formulated the following strategy for fitting a new force field that is capable of treating both silica and germania phases with minimal compromise inflicted by the requirements of the other phase. The short-range

Table 3. Interatomic Potential Parameters for Zeolites with Si,Ge as Tetrahedral Atoms

Atomic Charges

atom	core	shell
Si	4.0	-
Ge	4.0	-
O in Ge−O−Ge	1.733957	−3.733957
O in Si−O−Si	0.870733	−2.870733
O in Ge−O−Si	1.330431	−3.330431

Buckingham

i	j	A_{ij} (eV)	ρ_{ij} (Å)	C_{ij}(eV Å^6)
O shell	O shell	22764.0	0.149000	10.937044
Si core	O shell	1315.2478	0.317759	10.141118
Ge core	O shell	1497.3996	0.325646	16.808599

Three Body

i	j	k	k_{ijk} (eV rad^{-2})	θ_0(deg)
O shell	Si core	O shell	1.2614	109.47

Spring

i	j	k_{ij}^{cs}(eV Å^{-2})
O(Ge−O−Ge) core	O(Ge−O−Ge) shell	180.31577
O(Si−O−Si) core	O(Si−O−Si) shell	75.96980
O(Ge−O−Si) core	O(Ge−O−Si) shell	128.14279

Table 4. Atomic Charges for the Templates Used in the Synthesis of Octadecasil, ASU-7, and ASU-9

atom[a]	quinuclidine−H+	DMA−H+	DABCO−H+
N4	−0.5090	−0.6776	−0.3071
N3			−0.5180
C1	−0.0766	−0.1920	
C2	−0.1415		−0.0765
H	0.1739	0.2577	0.1757

[a] N4 and N3 are quaternary and tertiary nitrogen; C1 and C2 are primary and secondary carbon, respectively.

(34) Villaescusa, L. A.; Barrett, P. A.; Camblor, M. A. *Chem. Mater.* **1998**, *10*, 3966.
(35) Kiselev, A. V.; Lopatkin, A. A.; Shulga, A. *A. Zeolites* **1985**, *5*, 261.
(36) Oie, T.; Maggiora, T. M.; Christoffersen, R. E.; Duchamp, D. J. *Int. J. Quantum Chem., Quantum Biol. Symp.* **1981**, *8*, 1.
(37) Harrison, R.; Nichols, J.; Straatsma, T.; Dupuis, M.; Bylaska, E.; Fann, G.; Windus, T.; Apra, E.; Anchell, J.; Bernholdt, D.; Borowski, P.; Clark, T.; Clerc, D.; Dachsel, H.; de Jong, B.; Deegan, M.; Dyall, K.; Elwood, D.; Fruchtl, H.; Glendenning, E.; Gutowski, M.; Hess, A.; Jaffe, J.; Johnson, B.; Ju, J.; Kendall, R.; Kobayash, R.; Kutteh, R.; Lin, Z.; Littlefield, R.; Long, X.; Meng, B.; Nieplocha, J.; Niu, S.; Rosing, M.; Sandrone, G.; Stave, M.; Taylor, H.; Thomas, G.; van Lenthe, J.; Wolinski, K.; Wong, A.; Zhang, Z. *NWChem, A Computational Chemistry Package for Parallel Computers*, Version 4.0; Pacific Northwest National Laboratory, Richland, WA, 2000.
(38) Girard, S.; Gale, J. D.; Mellot-Draznieks, C.; Ferey, G. *J. Am. Chem. Soc.* **2002**, *124*, 1040.

O−O potential is constrained to remain the same within all phases, while the oxygen core−shell parameters are allowed to differ. This is achieved by concurrently fitting Ge-q, Ge-r, and Si-q, but with two distinct oxygen species defined for charges and the core−shell spring constant. To simulate the inclusion of one cation within the framework of the other (e.g., a Ge impurity in SiO_2), all that is necessary is to define the properties of each oxygen according to the types of atoms to which it is bonded. If an oxygen forms a Ge−O−Ge or Si−O−Si linkage, then the shell parameters appropriate to the pure phase are used. For an oxygen that lies in a Ge−O−Si environment, then the oxygen is defined according to the mean polarizability of the anion in germania and silica. This strategy is sufficient for energy minimization, where the discontinuity in type definition is not an issue. In contrast, for molecular dynamics a continuous energy surface is required with respect to bond breaking and formation. Hence, to extend the present approach to this scenario would require a minor modification by introducing smoothing functions that mix the polarizability according to the bond lengths and types of neighboring atoms. A similar approach is taken in some bond order models.[39] The concept of having two distinct oxygen types has been previously applied in the more extreme case of the oxygen−hydrogen interaction where hydroxyl groups are present. Although hydroxyl groups are often described as a molecular entity, with partial charges, Sierka and Sauer[40] have demonstrated that the use of distinct polarizabilities allows an ionic model to describe this situation.

As a consequence of the above approach, the oxygen−oxygen Buckingham term turned out to be different from that of previous work[30] and we lose here transferability of this force field to microporous structures containing Al and P. Further work to provide a wider force field that covers Si, Ge, Al, and P is underway based on the locally specific oxygen polarizability scheme presented here. By design, this method will be guaranteed to yield results equivalent to or better than existing force fields of the same functional form.

The quality of a fit can be measured by the sum of the squares of the differences between the experimental and calculated values for the observables, multiplied by appropriate weighting factors. Here, the weights used are 1000.0 for all unit cell parameters, 10 000.0 for all fractional coordinates, and 1.0 for all properties. This reflects the fact that there it is pointless to reproduce the curvature-related properties unless the structure is first reproduced. A final sum of squares of 29.2 is obtained within the above model. The values for the calculated properties with this interatomic potential are given in Table 2 and the interatomic potential parameters themselves are given in Table 3. Cell parameters of the Ge-q structure compare well to experimental values within a relative error of 0.2%, Ge−O distance is within a 1% error, and Ge−O−Ge angle is within 3° with respect to the experimental values. A previous model by Matsui et al.[24] reports cell parameters with similar accuracy to our force field with respect to the structural parameters of Ge-q, where a Ge−O distance of 1.744 Å, and a Ge−O−Ge angle of 134.1° are found. The bulk modulus for Ge-q (28.8 GPa) predicted by Matsui et al.[24] is slightly worse than our value of 37.7 GPa (see Table 2), which is closer to the experimental value of 36.0 GPa. For the Ge-r structure, the values of the bulk modulus are similar, as calculated in our model (243 GPa, see Table 2) and Matsui et al.,[24]the latter giving a slightly better value of 245 GPa, as compared to the experimental value of 258 GPa. The cell parameters of Ge-r are within 1% in the model by Matsui et al. and within 4% in our model. Regarding Ge−O distances, our model gives very good results within 0.5% with respect to the experimental values, and in Matsui et al.[24] are within 1% because of a slight underestimation of the second Ge−O distance which gives 1.890 Å. This shows that our model does not lose accuracy with respect to that of Matsui et al.[24] despite the fact of including the structure of SiO_2-quartz, which gives the possibility of including Si,Ge mixtures in the simulations. Regarding the magnitudes predicted for SiO_2-quartz, our model is of accuracy similar to that of the model by Sanders et al.[30a] which gives cell parameters of $a = 4.913$ Å and $c = 5.406$ Å, which are within 0.3%, and our values (Table 2) are also within an error of 0.3%. Elastic constants, static dielectric constants, and high-frequency dielectric constants are in good agreement with the experimental values (Table 2), although those reported by Sanders et al.[30a] are more accurate due to the fact that in our case the O−O term has been forced to take into account the three fitted structures.

3.2. Free Energy Minimization of the Structures of Ge-q and Ge-r. A study of the variation of free energy of the quartz and rutile polymorphs of germania with temperature has been undertaken in order to test whether the force field is able to reproduce the relative stability of these two phases. Free energy minimization has been performed within the zero static internal stress approximation,[41] where only the strains instead of all the internal degrees of freedom are minimized with respect to the free energy.[42] For each structure, the integration across the Brillouin zone of the phonon density of states has been performed using a Monkhorst−Pack grid, where shrinking factors are chosen to yield convergence in the free energy of at least six significant figures. For Ge-q, a shrinking factor of 6 was used along both the *a*/*b* and *c* axes, whereas the smaller cell dimensions of Ge-r necessitated the use of 6 and 10 for the same cell vectors, respectively. The free energy minimizations were performed over the temperature range 100−1800 K, with steps of 100 K, and the results are shown in Figure 1. The calculations were not continued above 1800 K because above this temperature the rutile phase develops imaginary modes that wish to lower the symmetry. This is an apparent contradiction often found within free energy calculations − increasing the temperature often drives low frequency modes close to zero, and ultimately imaginary, thus leading to lower symmetry, when experimentally materials are observed to become more symmetric. This occurs because low frequencies minimize the free energy

(39) Brenner, D. W.; Shenderova, O. A.; Harrison, J. A.; Stuart, S. J.; Ni, B.; Sinnott, S. B. *J. Phys. Condens. Matter* **2002**, 783.
(40) Sierka, M.; Sauer, J. *Faraday Discuss*. **1997**, *106*, 41.
(41) Taylor, M. B.; Barrera, G. D.; Allan, N. L.; Barron, T. H. K. *Phys. Rev. B* **1997**, *56*, 14380.
(42) Gale, J. D. *J. Phys. Chem. B* **1998**, *102*, 5423.

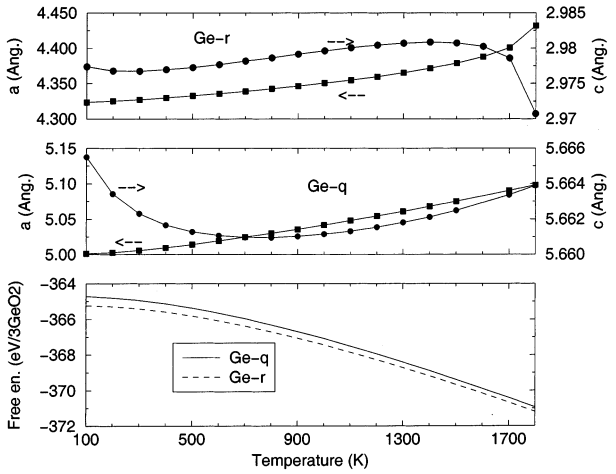

Figure 1. Results of the free energy minimizations of the Ge-q and Ge-r structures between 100 and 1800 K: bottom, free energy; middle, *a* and *c* cell parameters for Ge-q; top, *a* and *c* cell parameters for Ge-r.

in the statistical mechanical formalism based on the harmonic oscillator. However, since the distortion would be slight and the barrier low, there would be a dynamic process that jumps between the lower symmetry minima leading to an average structure that is symmetric.

It can be seen that the free energy of the rutile structure is always below that of Ge-q and that no phase change is observed within this temperature range although the phase change is experimentally observed at 1280 K.[8] Nevertheless, the right trend of decreasing relative stability of Ge-r with respect to that of Ge-q is observed, which amounts to 0.52 eV at 100 K and 0.25 eV at 1800 K. Furthermore, the greater stability of the rutile phase is correctly predicted by the calculations under ambient conditions. Phase transitions are notoriously difficult to reproduce correctly within potential models because a small error in the energy difference can lead to a large error in the temperature of transition. The addition of a three-body potential could be used, in principle, to reduce the energy difference between the phases, if the parameters were chosen to favor the tetrahedral angle. However, this is an artificial bias and has not been used here. It should be noted that the partial charge model of Matsui et al.[24] yields a smaller energy difference of 0.39 eV, which indicates that the degree of ionicity may be the most influential factor. Although in the quartz phase the shell model can mimic charge transfer, in the rutile analogue quadrupolar polarizability is required to achieve this.

The variations with temperature of the cell parameters *a* and *c* are illustrated in Figure 1 for the Ge-q phase (note that $a = b$ for all structures by symmetry). Although the variation of the *a* parameter shows regular positive thermal expansion, as would be expected, the *c* axis initially contracts on heating at low temperatures before eventually expanding. Negative thermal expansion is know to occur within some zeolitic materials[43] as a result of rigid unit modes. However, this is not observed to be the case for dense polymorphs, such as quartz. Therefore it is likely that the initial contraction along the *c* axis is an artifact of inaccuracies in the low frequency region of the phonon density of states, particularly with respect to how modes are coupled to atomic displacements, though there are no experimental data to conclusively indicate what the thermal expansion behavior of the polymorph should be. The rutile phase of GeO_2 demonstrates similar thermal expansion trends, despite the different structure, in that the *a* parameter expands regularly while the *c* parameter undergoes an initial contraction. After reverting to positive thermal expansion, the Ge-r phase eventually shows a collapse of the *c* axis with increasing temperature as the harmonic model for the free energy breaks down. Overall, we can postulate that the model may not be suitable for free energy minimization, based on the properties of silica analogues, though we will have to await the report of experimental or ab initio data on the thermal properties of germania polymorphs before we can be sure whether our predictions are valid or not.

3.3 Force Field Testing with Octadecasil, ASU-7, and ASU-9 Zeotypes. *3.3.1 Octadecasil.* This is an all silica ($Si_{20}O_{40}$) counterpart of the AlPO-16 structure[44] built up by linking octadecahedra [$4^6 6^{12}$] cages through all their common six-membered ring faces, and where D4Rs appear as the spacer between the linked cages. The structure has been solved in the space group *I*4/*m*.[33] When the template is used in the calculations, the final minimized structure gives cell parameters within 2% of the experimental values. The agreement with experiment for the average bond lengths and angles is also quite remarkable, particularly considering the uncertainty regarding the template-framework force field. The Si−O distances, for example, are within 0.7% of the experimental values, which corresponds to about 0.01 Å. Calculated Si−O−Si angles deviate less than 4° with respect to the experimental ones, and O−Si−O angles deviate less than 3°. The results are shown in Table 5.

Octadecasil has also been solved in the calcined form[34] and the agreement between experimental and calculated structures is also quite close, with errors of 2.3% and 0.5% in the cell parameters *a* and *c*, respectively. The Si−O distances are within 0.01 Å as in the previous case, while Si−O−Si angles are within 2°, and O−Si−O angles are within 1°, which is an excellent level of agreement. The results are given in detail in Table 6.

3.3.2. ASU-7. This is a germania structure ($Ge_{20}O_{40}$) solved by XRD in the tetragonal space group *P*4/*mcc* with cell parameters $a = 8.7795$ Å, $c = 14.4696$ Å, which are within 1.5% of the calculated values (see Table 7). The calculated and experimental structures are compared in Figure 2. The Ge−O distances are overestimated in the calculations by about 0.03 Å, which implies an error of 1.5%, although the experimental Ge−O distances vary between 1.69 and 1.74 Å, which seems too great a range, and further refinement of the structure may yield distances closer to each other. The calculated distances vary between 1.71 and 1.73 Å and this looks like a very reasonable range considering topological and strain factors. The Ge−O−Ge angles are very similar to the experimental values, as can be seen from $Ge_1-O_1-Ge_2$ (126.3° and 129.7°, experimental and calculated, respectively) and the other two: Ge_2-O_3-

(43) Couves, J. W.; Jones, R. H.; Parker, S. C.; Tschaufeser, P.; Catlow, C. R. A. *J. Phys. Condens. Matter* **1993**, *5*, 329.

(44) Bennett, J. M.; Kirchner, R. M. *Zeolites* **1991**, *11*, 502.

Table 5. Comparison of the Octadecasil Structures from XRD[33] and Calculated with the Force Field in Table 3 for the As-Synthesized Materials with Quinuclidine[a]

cell parameter	experimental	calculated
a	9.194	9.043
b	9.194	9.039
c	13.396	13.434

T−O label	T−O (exp)	T−O (calc)	number
Si1 O2	1.612	1.623	32
Si1 O3	1.617	1.625	16
Si1 O1	1.612	1.610	16
Si2 O1	1.606	1.607	16

T−T label	T−T (exp)	T−T (calc)	number
Si1 Si1	3.040	3.029	24
Si1 Si2	3.100	3.065	16

T−O−T label	T−O−T (exp)	T−O−T (calc)	number
Si1 O2 Si1	140.8	137.8	16
Si1 O3 Si1	140.7	137.3	8
Si1 O1 Si2	148.8	144.7	16

O−T−O label	O−T−O (exp)	O−T−O (calc)	number
O1 Si1 O2	106.0	104.3	32
O1 Si1 O3	104.8	103.5	16
O2 Si1 O2	113.6	115.1	16
O2 Si1 O3	112.7	114.1	32
O1 Si2 O1	109.5	109.5	24

[a] All distances in Angstroms and angles in degrees.

Table 6. Comparison of the Octadecasil Structures from XRD[34] and Calculated with the Force Field in Table 3 for the Calcined Materials[a]

cell parameter	experimental	calculated
a	9.255	9.043
b	9.255	9.039
c	13.501	13.434

T−O label[b]	T−O (exp)	T−O (calc)	number
Si1 O2	1.609	1.609	32
Si1 O3	1.604	1.609	16
Si1 O1	1.607	1.593	16
Si2 O1	1.589	1.600	16

T−T label	T−T (exp)	T−T (calc)	number
Si1 Si1	3.082	3.091	24
Si1 Si2	3.099	3.105	16

T−O−T label	T−O−T (exp)	T−O−T (calc)	number
Si1 O2 Si1	147.2	147.9	16
Si1 O3 Si1	146.5	147.6	8
Si1 O1 Si2	151.7	153.1	16

O−T−O label	O−T−O (exp)	O−T−O (calc)	number
O1 Si1 O2	108.8	109.1	32
O1 Si1 O3	108.6	108.9	16
O2 Si1 O2	110.5	109.9	16
O2 Si1 O3	110.0	109.9	32
O1 Si2 O1	109.5	109.5	24

[a] All distances in Angstroms and angles in degrees. [b] The same oxygen labeling as that from Caullet et al.[33] has been used for the sake of comparison with Table 5.

Ge_2, and $Ge_2-O_2-Ge_2$, which are within 1° of each other, in excellent agreement with the experimental values, as can be seen from Table 7. Furthermore, calculated O−Ge−O angles are within 1° of the experimental ones.

3.3.3. ASU-9. This is also a germania structure ($Ge_{20}O_{40}$) isostructural to octadecasil and solved by XRD

Table 7. Comparison of the ASU-7 Structure from XRD[13] and Calculated with the Force Field in Table 3 for the As-Synthesized Materials with Dimethylamine[a]

cell parameter	experimental	calculated
a	8.7795	8.7183
b	8.7795	8.7659
c	14.4696	14.6854

T−O label	T−O (exp)	T−O (calc)	number
Ge1 O1	1.741	1.731	16
Ge2 O1	1.750	1.726	16
Ge2 O3	1.698	1.720	32
Ge2 O2	1.690	1.718	16

T−T label	T−T (exp)	T−T (calc)	number
Ge1 Ge2	3.115	3.129	16
Ge2 Ge2	3.159	3.201	24

T−O−T label	T−O−T (exp)	T−O−T (calc)	number
Ge O1 Ge2	126.3	129.7	16
Ge2 O3 Ge2	137.8	137.6	16
Ge2 O2 Ge2	136.9	136.2	8

O−T−O label	O−T−O (exp)	O−T−O (calc)	number
O1 Ge2 O1	109.6	109.6	24
O1 Ge2 O2	105.2	105.8	16
O1 Ge2 O3	103.4	103.1	32
O2 Ge2 O3	114.8	113.8	32
O3 Ge2 O3	113.4	115.4	16

[a] All distances in Angstroms and angles in degrees.

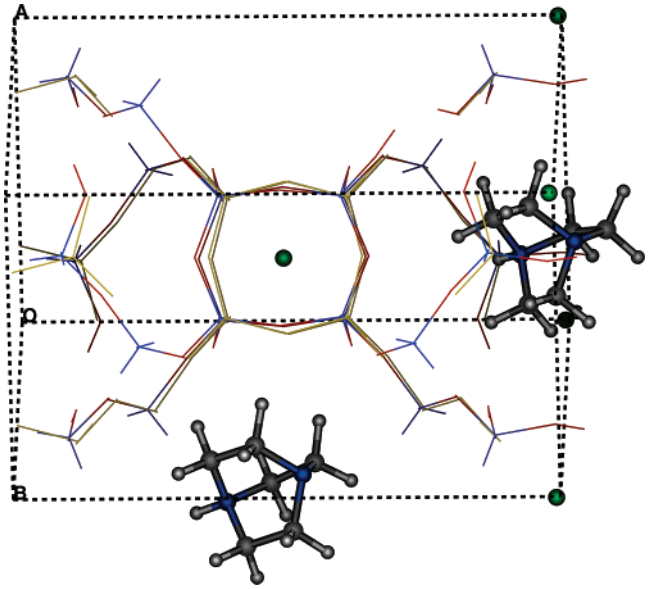

Figure 2. Comparison of the calculated and experimental crystal structures of ASU-9. The calculated structure is in red/blue, and the experimental structure is in monochrome.

in the space group *I*4/*m* with cell parameters $a = 9.2314$ Å, $c = 14.0960$ Å, which lie within 1% of the calculated ones (see Table 8 and Figure 3). The agreement between the experimental and calculated Ge−O is within 0.038 Å, which is reasonable, although the same consideration as in the previous structure applies, and experimental values ranging from 1.68 to 1.74 Å seem slightly unlikely, whereas the range 1.720−1.724 Å is observed within the calculated Ge−O distances. The Ge−O−Ge angles are now within 5° of experiment, which is a more significant discrepancy, but again the O−Ge−O values are within 1° of the observed values (Table 8).

Table 8. Comparison of the ASU-9 Structure from XRD[13] and Calculated with the Force Field in Table 3 for the As-Synthesized Materials with DABCO[a]

cell parameter	experimental	calculated
a	9.2314	9.2081
b	9.2314	9.1559
c	14.0960	14.2319

T−O label[b]	T−O (exp)	T−O (calc)	number
Ge1 O2	1.688	1.722	32
Ge1 O3	1.683	1.721	16
Ge1 O1	1.741	1.724	16
Ge2 O1	1.730	1.720	16

T−T label	T−T (exp)	T−T (calc)	number
Ge1 Ge1	3.155	3.169	24
Ge1 Ge2	3.177	3.178	16

T−O−T label	T−O−T (exp)	T−O−T (calc)	number
Ge1 O2 Ge1	138.1	133.7	16
Ge1 O3 Ge1	139.9	134.5	8
Ge1 O1 Ge2	132.5	134.7	16

O−T−O label	O−T−O (exp)	O−T−O (calc)	number
O1 Ge1 O2	105.4	105.5	32
O1 Ge1 O3	103.9	103.5	16
O2 Ge1 O2	114.1	114.8	16
O2 Ge1 O3	112.9	113.5	32
O1 Ge2 O1	109.5	109.5	24

[a] All distances in Angstroms and angles in degrees. [b] The same oxygen labeling as that from Caullet et al.[33] has been used for the sake of comparison with Table 5.

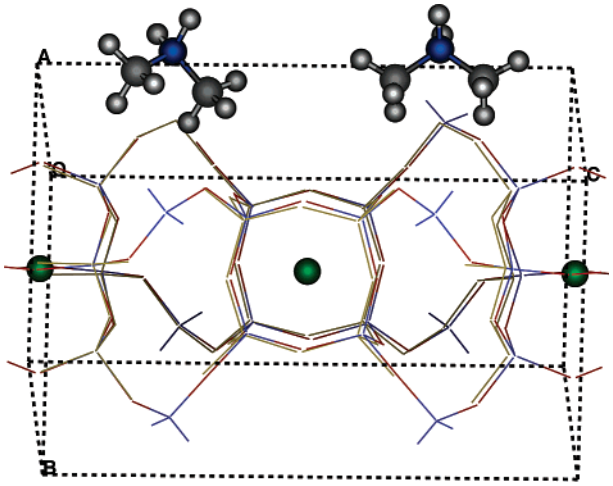

Figure 3. Comparison of the calculated and experimental crystal structures of ASU-7. Color scheme is the same as that in Figure 2.

3.4. Application of the Force Field to a Mixed Si/Ge Structure: Ge−ITQ-7. As a first example of the potential application of the force field we have considered the material ITQ-7 in which germanium has been partially incorporated into the framework. ITQ-7[4] is a zeolite with three interconnected channel systems of 12 MR (membered ring): two of them are of the same size and shape (6.2 × 6.1 Å) and run along the directions [100] and [010]. The third 12 MR system runs parallel to [001] and is formed by windows of 6.3 × 6.1 Å. The refined tetragonal $P4_2/mmc$ structure of pure silica ITQ-7 was used as a starting point and then a single Ge atom was introduced in the unit cell. Four molecules of the structure-directing agent used in the synthesis (1,3,3-trimethyl-6-azonium-tricyclo[3.2.1.4^{6,6}] dodecane hydroxyde),[5] as well as four fluorine atoms, have been considered in the calculation (see Figure 4). A methodology similar to that in a previous study has been employed for the calculations.[45] The fluorine atoms were located inside the double four ring (D4R) units as observed experimentally.[4] Five different calculations were run, corresponding to the Ge atom located in each of the 5 tetrahedral positions of the ITQ-7 structure (Figure 4). Although the results must be considered preliminary, because more work is required to establish an optimal force field for fluoride ions in the present phase, it is found that the calculations (Table 9) show a preference for incorporation of Ge into the T1 and T4 positions, which correspond to atoms in D4R units. This result is in agreement with the interpretation of the results obtained by NMR techniques in a previous experimental study.[19]

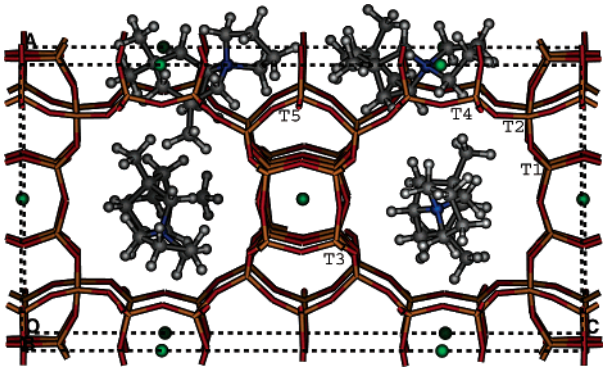

Figure 4. Structure of ITQ-7 showing the 5 different T sites, the structure-directing agent used in the synthesis ($C_{14}H_{26}$-NOH), and the four fluorine atoms present in the unit cell.

Table 9. Calculated Energy (kJ/mol) for the Incorporation of Ge in ITQ-7 Zeolite Relative to the Most Stable Site

T site	relative energy (kJ/mol)[a]
T1	0.0
T2	48.2
T3	59.8
T4	1.0
T5	65.6

[a] Four molecules of the structure-directing agent, as well as four fluorine atoms, have been taken into account in the calculations which have been performed at constant volume.

4. Conclusions

A new force field has been derived that is able to model the 4-fold and 6-fold coordination environments of Ge, although it is primarily intended to be used in the tetrahedral coordination typical of zeotypes. The present work manages to improve on the results of previous shell model parametrizations through the use of distinct polarizabilities for oxygen according to the elements to which it is bonded. This appears to be essential if the geometric features of both quartz and the germania analogue are to be faithfully reproduced. The main structural features of germanium in zeolites are also faithfully reproduced by this force field and

(45) Sastre, G.; Fornes, V.; Corma, A. *J. Phys. Chem. B* **2002**, *106*, 701.
(46) Sastre, G.; Gale, J. D. *Microporous Mesoporous Mater.* **2001**, *43*, 27.

interatomic distances for Ge−O within the range of 1.71−1.73 Å are obtained, in good agreement with the mean of the experimental data from the two first zeotypic germanates synthesized, ASU-7 and ASU-9, though with a narrower distribution. The same can be said of the Ge−O−Ge angles, with values calculated to lie within the range of 130−138° in close concordance with experiments, which show a range of 126−140°. Furthermore, O−Ge−O angles are close to the experimentally reported values with a typical deviation of less than 2°. On the other hand, the Si part of the force field does not lose accuracy when simulating all-silica frameworks with respect to previous force fields, as demonstrated from the results obtained for octadecasil which show cell parameters within 2%, Si−O distances within 1%, and Si−O−Si angles within 2° with respect to the experimentally reported values.

Energetically, the force field predicts the correct order of stability between 6-fold and 4-fold coordinated phases of germania. However, the rutile-structured polymorph appears to be overstabilized with respect to the quartz analogue, as the phase transition is predicted to occur at temperatures higher than that observed experimentally. Nevertheless, the force field would be capable of modeling germanium environments within zeolitic frameworks where the coordination number is increased beyond four due to the binding of extra species, as it observed for aluminum. Finally, this force field is expected to be of particular utility when applied to Ge/Si mixed structures and can be employed as a tool to calculate the preferential cation ordering, as well as related structural features. Both of these aspects will be investigated in future work, as will the development of consistent parameters for the treatment of aluminophosphate materials in order to maximize the chemical variety that can be studied with the new force field.

Acknowledgment. G.S. thanks Generalitat Valenciana (project GV01-492) for financial support, and C^4 (Centre de Computacio i Comunicacions de Catalunya) for the use of their computer facilities. The High Performance Computational Chemistry Group from Pacific Northwest National Laboratory (Richland, WA), is acknowledged for making available NWChem version 4.0, a computational chemistry package for parallel computers. J.D.G. thanks EPSRC for funding of computer facilities.

CM021262Y